HHS Public Access

Author manuscript

Mucosal Immunol. Author manuscript; available in PMC 2013 May 01.

Published in final edited form as:

Mucosal Immunol. 2012 November ; 5(6): 691–701. doi:10.1038/mi.2012.42.

Regulatory B Cells from Hilar Lymph Nodes of Tolerant Mice in a Murine Model of Allergic Airway Disease are CD5+, Express TGF-β and Co-localize with CD4+Foxp3+ T Cells

Prabitha Natarajan[1], **Anurag Singh**[1,2], **Jeffrey T. McNamara**[1], **Eric R. Secor Jr**[1], **Linda A. Guernsey**[1], **Roger S. Thrall**[1], and **Craig M. Schramm**[3]

[1]Department of Immunology, University of Connecticut Health Center, Farmington, CT 06030 [2]Nestle Research Center, Vers-chez-les-Blanc, CH-1000, Lausanne 26, Switzerland [3]Department of Pediatrics, University of Connecticut Health Center, Farmington, CT 06030

Abstract

In a biphasic, ovalbumin (OVA)-induced murine asthma model where allergic airway disease is followed by resolution and the development of local inhalational tolerance (LIT), TGFβ-expressing $CD5^+$ B cells were selectively expanded locally in hilar lymph nodes (HLN) of LIT mice. LIT HLN $CD5^+$ B cells but not LIT HLN $CD5^-$ B cells induced expression of Foxp3 in $CD4^+$ $CD25^-$ T cells *in vitro*. These $CD5^+$ regulatory B cells and $CD4^+Foxp3^+$ T cells demonstrated similar increases in expression of chemokine receptors (CXCR4 and CXCR5) and co-localized in HLN B cell zones of LIT mice. The adoptive transfer of LIT HLN $CD5^+$ B cells, but not LIT HLN $CD5^-$ B cells, increased the number of $CD4^+Foxp3^+$ T cells in the lung and inhibited airway eosinophilia in this OVA model. Thus, regulatory B cells in HLNs of LIT mice reside in a $CD5^+$ TGFβ-producing subpopulation and co-localize with $CD4^+Foxp3^+$ T cells.

Keywords

asthma; B lymphocytes; $Foxp3^+$; T lymphocytes

INTRODUCTION

Research over the last three decades has provided overwhelming evidence that asthma is an inflammatory disease of the airways orchestrated by T lymphocytes.[1,2] Activation of Th2 effector lymphocytes (Teff) causes elaboration of cytokines such as IL-4, IL-5, and IL-13, which in turn results in eosinophil activation and IgE production intrinsic to allergic

*Corresponding Author: Craig M. Schramm, M.D., Pulmonary Division, Connecticut Children's Medical Center, 282 Washington Street, Hartford, CT 06106 USA, Tel: 860-545-9440, FAX: 860-545-9445, schramm@neuron.uchc.edu.

SUPPLEMENTARY MATERIAL is linked to the online version of the paper at http://www.nature.com/mi.

DISCLOSURE

The authors declared no conflict of interest.

inflammation.[3,4] The identification of regulatory T lymphocytes (Tregs) that can modulate Teff function has led to intensive research on their role in allergic asthma.[5–7] B lymphocytes have traditionally been viewed as target cells for Th2 cytokines, with IL-4 and IL-13 responsible for the initiation and maintenance of B cell IgE production.[8] However, emerging evidence suggests that there are also regulatory types of B cells (Bregs), which are specifically induced under inflammatory conditions[9–14] and which are capable of suppressing inflammation, enhancing recovery, or inducing tolerance.[15–17] Such Bregs have been implicated in the development of nasal tolerance to aeroallergens.[18] Like Tregs, Bregs may comprise several subpopulations that exhibit different mechanisms of immunomodulation, including production of anti-inflammatory cytokines (IL-10 or TGF-β1), function as inhibitory antigen presenting cells, and induction or recruitment of Tregs.[19,20]

We have recently identified a novel putative Breg that may be involved in the regulation of airway inflammation.[21] Acute aerosolized ovalbumin (OVA) exposure in sensitized mice induces typical allergic airway disease (AAD), but chronic inhalational antigen exposure results in resolution of the airway eosinophilia, Th2-cytokine secretion, and airway hyperreactivity[22–27] regardless of the persistence of OVA-specific IgE in serum and OVA-specific subcutaneous allergic reactions.[23,28] Reflecting the focal resolution of inflammation, we have termed this process local inhalational tolerance (LIT). Adoptive transfer of regional hilar lymph node (HLN) B cells from LIT mice to OVA-sensitized recipients increases the number of $CD4^+CD25^+Foxp3^+$ Tregs in BAL and attenuates AAD following subsequent OVA aerosol exposure.[21] In contrast to AAD HLN B cells or LIT splenic B cells, LIT HLN B cells produce TGF-β and are capable of converting naïve $CD4^+CD25^-$ T cells into functionally suppressive $CD4^+CD25^+Foxp3^+$ regulatory T cells ($Foxp3^+$ Treg) *in vitro*.[21] These findings discovered a regulatory role for regional B cells in the attenuation of inflammation and re-establishment of homeostasis in the airway despite ongoing antigen challenge. The present study was undertaken to further establish the phenotype of these TGFβ-producing Bregs and to investigate their relationship to Tregs in respect to location in the HLN and in chemokine receptor expression.

RESULTS

$CD5^+$ B cells were increased in the HLN at AAD and LIT

B cells isolated from inguinal lymph nodes and spleens were found to have an identical phenotype in both AAD and LIT mice: $CD21^{interm}IgD^{hi}$ $IgM^{interm}CD5^{lo}$, consistent with mature follicular B cells. AAD HLN B cells had a similar phenotype to the cells in these systemic tissues, whereas LIT HLN had increased percentage of IgD^{lo} and $CD5^{hi}$ cells as compared to AAD (Supplementary Figure S1). In hilar lymph nodes, there was a significant increase ($p < 0.005$) in the total number of $CD5^+$ B cells in mice at AAD and LIT as compared to mice in the Naïve and Sensitized groups and to any of the groups in inguinal lymph nodes (Figure 1A). In the inguinal nodes, there were no significant differences in the total number of $CD5^+$ B cells in mice at any of the stages (Figure 1A). Also in the HLN, there was a significant increase ($p < 0.005$) in the percentage $CD5^+$ B cells in mice at LIT as compared to mice in the Naïve, Sensitized and AAD groups and to any of the groups in

inguinal nodes (Figure 1B). In contrast, in the inguinal lymph nodes, there were no significant differences in the percentage of $CD5^+$ B cells in mice at any of the stages (Figure 1B).

LIT HLN $CD5^+$ B cells predominantly expressed TGF-β

The selective expansion of $CD5^+$ B cells in HLNs from LIT mice suggested that these cells could constitute the suppressive Breg phenotype identified previously, where B lymphocytes isolated from HLNs of LIT mice induced $CD4^+CD25^+Foxp3^+$ T cells via expression of TGF-β.[21] Thus, we examined whether the LIT HLN TGFβ-producing B cells resided in the $CD5^+$ or $CD5^-$ cell population. Minimal LAP expression was seen in $CD5^+$ or $CD5^-$ cells isolated from spleens of Naïve or LIT mice (0.08–0.2% of these B cells were LAP^+; Figure 2A and 2C). LAP was found at low levels in both types of B cells from HLN of Naïve mice. Its expression increased in both $CD5^+$ and $CD5^-$ B cells in HLN from LIT mice, but the enhanced expression was much more dramatic in the $CD5^+$ LIT HLN B cell population. In LIT HLNs, 37.9 ± 9% of $CD5^+$ B cells were LAP^+, as compared to 13.3 ± 4% of $CD5^-$ B cells ($p < 0.05$; Figure 2C). As anticipated, little IL-10 staining was seen in unstimulated B cells, but IL-10 production could be induced by 5-hour stimulation with phorbol 12-myristate 13-acetate and ionomycin.[29] As shown in Figures 2B and 2D, IL-10 was also primarily produced by $CD5^+$ B cells (8.2 ± 1.3% in LIT HLN and 5.2 ± 0.7% in LIT spleen) as compared to $CD5^-$ B cells (1.0 ± 0.3% in LIT HLN and 0.6 ± 0.1% in LIT spleen; $p < 0.0005$ each). Unfortunately, the LAP staining was poor in these studies, possibly because of interference from the IL-10 staining conditions (e.g., permeabilization, low temperature), and so co-expression of IL-10 and TGF-β could not be directly assessed. However, in contrast to TGF-β, IL-10 production did not differ between LIT HLN and LIT spleen $CD5^+$ B cells ($p > 0.05$), and in the HLNs, $CD5^+$ B cell expression of IL-10 was significantly less than their expression of TGF-β ($p < 0.005$; Figure 2D).

LIT HLN $CD5^+$ B cells induced formation of $Foxp3^+$ T cells *in vitro*, and adoptive transfer of LIT HLN $CD5^+$ B cells increased airway $Foxp3^+$ Tregs in sensitized recipient mice

We have previously demonstrated that LIT HLN B cells can induce Foxp3 expression in naïve T cells *in vitro* through a mechanism dependent on TGF-β and independent of IL-10.[21] To determine if the differential expression of LAP/TGF-β in $CD5^+$ versus $CD5^-$ HLN B cells resulted in functional distinctions in the two subsets, $CD19^+$ B cells that were isolated from HLNs of LIT mice were divided into $CD5^+$ and $CD5^-$ populations, irradiated, and then co-cultured with naïve splenic $CD4^+CD25^-$ T cells and anti-CD3/CD28. $Foxp3^+$ expression by the T cells was increased 3-fold by LIT HLN $CD5^+$ B cells relative to control stimulated conditions, but the LIT HLN $CD5^-$ B cells were without effect (Figure 3A). B cells were also required for the *in vivo* expansion of $Foxp3^+$ Treg cells during LIT. In a first series of experiments, the progression of AAD to LIT was compared in wildtype mice and in B-cell-deficient $JhD^{-/-}$ mice (Jackson Laboratory, Bar Harbor, ME). Wildtype mice showed regional expansion of $Foxp3^+$ T cells during LIT, occurring in hilar but not inguinal lymph nodes (Figure 3B). This regional expansion did not occur in the $JhD^{-/-}$ mice (Figure 3B; $p < 0.005$ vs. wildtype mice). Next, adoptive transfer studies were performed with LIT HLN $CD5^+$ B cells, LIT HLN $CD5^-$ B cells, and LIT Spleen $CD5^+$ B cells. The number of airway $Foxp3^+$ Tregs present in bronchoalveolar lavage of AAD mice increased by 43% in mice

receiving LIT HLN $CD5^+$ B cells ($0.70 \pm 0.1 \times 10^5$ cells) as compared to saline control mice ($0.5 \pm 0.1 \times 105$ cells) but was not affected by the adoptive transfer of LIT HLN $CD5^-$ B cells or LIT splenic $CD5^+$ B cells (Figure 3C). Moreover, there was a direct correlation between the number of airway $Foxp3^+$ Tregs and airway $CD5^+$ B cells ($r = 0.56$; $p < 0.005$; Figure 3D). This correlation did not hold between airway $Foxp3^-$ Teff cells and $CD5^+$ B cells in ($r = 0.27$; $p = 0.20$) or between airway $Foxp3^+$ Tregs and $CD5^-$ B cells ($r = 0.31$; $p = 0.14$; data not shown).

$Foxp3^+$ Tregs increased in the B cell zone and T cell - B cell border of hilar lymph nodes via confocal microscopy in mice at LIT

The expansion of airway and HLN $Foxp3^+$ cells from AAD to LIT was associated with a striking difference in the distribution of $Foxp3^+$ Tregs in HLNs, as demonstrated in representative confocal microscopy images in Figure 4A–4C. Qualitative observations of these confocal images showed apparent increases of $Foxp3^+$ Tregs in HLN of mice at LIT (Figure 4A, lower panel) as compared to sensitized and AAD stages (Figure 4A, upper and middle panels). These observations were supported by quantification of $Foxp3^+$ Tregs and B cells in different compartments of the HLN, which included T cell zone, T cell - B cell border (T-B border), and B cell zone (follicle). Representative images for the quantification strategy of $Foxp3^+$ Tregs in the T-B border are shown in Figures 4B and 4C. In general, the B cell zones (follicular area) were reduced in size and number of cells in the HLN at LIT as compared to AAD, corresponding with the resolution of lung inflammation (Supplementary Table 1). There was a 78.3% increase ($p < 0.05$) in the density of Tregs (follicular Tregs) in the follicular B cell zone of HLN from mice at LIT as compared to AAD (Figure 4D), with no changes in $Foxp3^+$ Treg densities in the T cell zone and T-B border. Moreover, in the T-B border and B cell zone, the ratios of $Foxp3^+$ Tregs to B cells increased 184% and 146%, respectively, in HLN from mice at LIT as compared to AAD (Figure 4E; $p < 0.05$ each). Thus, $Foxp3^+$ Tregs preferentially localized in the follicular area of the HLN at LIT. CD5 staining was not bright enough to permit specific identification of $CD5^+$ B cells by confocal microscopy.

The number of $CD5^+$ B cells and $Foxp3^+$ Tregs expressing CXCR4 and CXCR5 were increased in the HLN at AAD and LIT

The co-localization of B cells and $Foxp3^+$ T cells in HLNs suggested that the cells could be expressing similar chemokine receptors. Therefore, the expression of CXCR4 and CXCR5 on $CD5^+$ B cells and Tregs was compared between hilar and inguinal lymph nodes and at various stages of the OVA model (Naïve, Sensitized, AAD and LIT). Significantly more $CD5^+$ B cells expressed CXCR4 in hilar nodes versus inguinal nodes at each stage of the model ($p < 0.05$; Figure 5B), and this regional expression increased further at AAD and LIT as compared to Naïve and Sensitized stages ($p < 0.05$). Moreover, within hilar lymph nodes, expression of $CXCR4^+$ was 2.3- to 3.5-fold higher on $CD5^+$ B cells than on $CD5^-$ B cells at all stages of the model (Supplementary Figure S3). No changes were observed in the percentage of $CXCR4^+$ $CD5^+$ B cells in the inguinal lymph nodes except for a significant decrease at the Sensitized stage. There was no difference in the percentage of $CD5^+$ B cells expressing CXCR5 at any of the stages in hilar or inguinal lymph nodes (Figure 5C). Like the percentages, the total number $CD5^+$ B cells expressing CXCR4 was significantly

increased in the HLN of mice at AAD and LIT as compared to mice at Naïve and Sensitized stages (Supplementary Figure S2A), and the total number of $CD5^+$ B cells expressing CXCR5 was also increased at AAD and LIT (Supplementary Figure S2B). The number of $CD5^+$ B cells expressing CXCR4 and CXCR5 was not altered in the inguinal lymph node at any of the stages (Supplementary Figure S2A and S2B).

The percentage (Figure 6B) and total number (Supplementary Figure S2C) of $Foxp3^+$ Tregs expressing CXCR4 were also increased in the hilar nodes in mice at AAD and LIT, as compared to Naïve and Sensitized groups ($p < 0.005$), with no changes seen in inguinal nodes. In contrast to $CD5^+$ B cells in the HLN, the percentage of $Foxp3^+$ Tregs expressing CXCR5 was significantly increased in mice at AAD and LIT as compared to Naïve and Sensitized stages ($p < 0.005$; (Figure 6C). In inguinal nodes, the percentage of $CXCR5^+$ $Foxp3^+$ Tregs was not altered at any of the stages (Figure 6C). Similarly, the total number of Tregs expressing CXCR5 was significantly increased in HLNs of mice at AAD and LIT as compared to mice in Naïve and Sensitized stages (Supplementary Figure S2D). These data show that both $CD5^+$ B cells and $Foxp3^+$ Tregs up-regulate the expression of CXCR4 and CXCR5 at AAD and LIT specifically in hilar but not inguinal lymph nodes.

Adoptive transfer of LIT HLN $CD5^+$ B cells attenuated airway eosinophilia in sensitized recipient mice

The association between $CD5^+$ B cells and $Foxp3^+$ Tregs suggested that the regional HLN B cells responsible for the previously reported attenuation of AAD[21] resided in the $CD5^+$ population. To test this, the degree of AAD was compared in animals receiving LIT HLN $CD5^+$ B cells and animals receiving other cells. The development of airway eosinophilia was significantly reduced in mice that received LIT HLN $CD5^+$ B cells ($60.6 \pm 2.0\%$ and $17.2 \pm 2.6 \times 10^5$ eosinophils) as compared to mice that received either vehicle alone, LIT HLN $CD5^-$ B cells or LIT spleen $CD5^+$ B cells (Figure 8). Mice receiving LIT spleen $CD5^-$ B cells, naïve spleen $CD5^-$ B cells, or naïve spleen $CD5^+$ B cells also developed similar airway eosinophilia as the control recipient animals (data not shown).

DISCUSSION

Previously we have shown that regional B cells isolated from hilar lymph nodes of LIT mice are capable of suppressing AAD in recipient animals.[21] B cells from LIT HLNs are unique in this function, as AAD suppression is not exerted by B cells isolated from AAD HLN or by splenic B cells of either AAD or LIT mice.[21] These LIT HLN Bregs induce $Foxp3^+$ T cell generation through expression of TGF-β.[21] The present study further characterized these Bregs as a specific local $CD19^+B220^+CD1d^{hi}CD5^+$ B cell population expressing TGF-β and up-regulated expression of the chemokine receptor CXCR4.

The finding of $CD5^+$ cells in LIT HLNs was distinctive, as there are very few reports of $CD5^+$ cells in draining lymph nodes.[30] Their presence, in part, could be attributed to their expression of the chemokine receptors CXCR4 and CXCR5. The high level of CXCR5 expression by all the hilar and inguinal node B cells was consistent with its constituitive expression on circulating B cells, which directs their homing to B-cell follicles.[31,32] The upregulation of CXCR4 on HLN $CD5^+$ B cells at AAD and LIT would direct their

localization to germinal center dark zones, which are located adjacent to T-cell areas.[33] Further, the observation of increased expression of CXCR4 and CXCR5 on HLN Foxp3$^+$ Tregs during AAD and LIT would facilitate their interaction with follicular B cells by placing Bregs and Foxp3$^+$ Tregs in close proximity in the hilar nodes. Foxp3$^+$ Treg cells are known to express CXCR4,[34] and so the increased numbers of CXCR4$^+$Foxp3$^+$ Treg cells in HLNs of AAD and LIT mice may have been due to enhanced migration of existing Foxp3$^+$ Treg cells to the HLN. Alternately, the ability of LIT HLN CD5$^+$ B cells to convert naïve CD4$^+$ T cells to suppressive Foxp3$^+$ Treg cells *in vitro* raises the intriguing possibility that this conversion may be occurring *in vivo* in the HLN follicles, initially during AAD to help limit the inflammatory response and continued at LIT to sustain the reestablished airway homeostasis. The confocal images support the close localization of these regulatory cells in the HLN especially in the T-B border, both qualitatively and quantitatively.

Other investigators have implicated a regulatory role for B-1a CD19$^+$CD5$^+$ cells in moderating allergic airway disease. In a cockroach allergen-induced asthma model, mice that are deficient in B-1a cells (CBA/CaHN-*Btk*^{xid}/J mice) develop higher serum IgE levels and more airway inflammation than wildtype mice.[35] It should be noted, however, that Xid mice have several B-cell abnormalities, including impaired survival of follicular IgD^{hi}IgM^{lo} B cells and reduced numbers of marginal zone B cells.[36] Thus, potential abnormalities in other regulatory B cell populations in Xid mice could have accounted for their increased allergic airway disease. The IgD^{lo}CD5^{hi} phenotype also suggested a B-1 rather than B-2 cell morphology in our subpopulation of LIT HLN B cells; however, all the cells were also B220$^+$ (e.g., CD45R^{hi}), which is associated with B-2 cells. Thus, the expanded population of CD19$^+$CD5$^+$ cells in LIT HLNs had characteristics of both B-1 (IgD^{lo}) and B-2 (B220$^+$) subsets, and therefore may reflect a previously undefined Breg cell population that arose with chronic antigen exposure. Indeed, while CD5 expression is characteristic of B-1 cells, this surface marker can also be induced in B-2 cells by a variety of stimuli.[37] CD5 expression can be induced in human peripheral blood B cells by co-cultivation with T cells via CD40-CD40L interaction, and these CD5+ B cells have T-cell suppressive activity.[38] Since our LIT mice are chronically exposed to OVA for 6 weeks, the CD5$^+$ cells seen in their HLN may represent induced expression of the marker by non-B-1 cells.

To date, most studies of regulatory B cells have focused on IL-10-producing B10 cells that reside in a CD19^{hi}CD1d^{hi}CD5$^+$ B-cell population.[39,40] It has been shown that B10 cells expand in response to *Schistosoma mansoni* infections, and that the adoptive transfer of these B10 cells into allergen-sensitized mice suppresses anaphylaxis and AAD through IL-10–dependent mechanisms.[41,42] These B10 cells have a CD19$^+$CD21^{hi}CD23$^+$IgD$^+$IgM^{hi}CD1d^{hi} phenotype,[42] somewhat similar to our CD19$^+$CD21^{interm}IgD^{lo}IgM^{interm}CD1d^{hi} LIT HLN B cells. In the worm model, these suppressive B10 cells were found in the spleen. We found some expansion of CD5$^+$ IL-10 producing B cells in the spleen and HLN in LIT mice (Figure 2D); however, these cells were ineffective at inhibiting AAD (Figure 7). In our LIT model, the suppressive Bregs arose only in regional HLNs, and no suppressive B cells were found in spleen or inguinal lymph node tissues. Moreover, the LIT hilar nodes contained 5-fold more TGF-β$^+$ cells than IL-10$^+$ cells (Figure 2). Of interest, CD19$^+$ B cells from regional, mesenteric lymph nodes of mice with

chronic enteric helminth infections are also capable of suppressing AAD through an IL-10–independent mechanism.[43] In addition, both IL-10 producing $CD19^+CD5^+$ B cells (B-10 cells) and TGFβ-producing $CD19^+CD5^+$ B cells have been shown to regulate cow's milk allergic responses in human subjects.[44, 45] TGFβ-expressing B cells have also been shown to down-regulate pathogenic Th1 immunity in nonobese diabetic mice.[14] As with T cells, it is likely that several populations of regulatory B cells exist, and that different subsets may be preferentially generated based on the types of stimuli and anatomical sites of antigen presentation.

Asthma is a complex disease. Its generation and resolution, pathogenesis and regulation are dependent upon intricate interactions between adaptive and innate immune cells. In animal models, antigen-induced AAD constitutes an unwanted and unnecessary Th2-driven inflammatory reaction against harmless inhaled antigens. LIT represents one process by which mice are able to suppress this detrimental inflammatory response and re-establish airway homeostasis despite ongoing systemic responses. It is apparent, both from basic science and clinical stand points, that no one cell type – effector or regulator – stands alone in this disease and is able to create or prevent asthma. Our studies have shown that LIT does not depend on the presence of either Bregs or $Foxp3^+$ Tregs in knockout or antibody-depleted animals.[21,46] Although B-cell knockout animals develop LIT, they do so despite diminished levels of regional $Foxp3^+$ Tregs. This finding supports the complex and interactive contributions of Bregs and Tregs in the development of tolerance in wildtype animals. Indeed, the contrasting pro- and anti-inflammatory roles of B and T cells are likely to overlap in asthma, with the balance of these opposing actions determining the natural course of the disease.

In summary, the present study identified a subpopulation of B cells that arose preferentially in regional lymphoid tissues in response to chronic antigen exposure and inflammation. These cells express a $CD19^+B220^+CD21^{interm}IgD^{lo}IgM^{interm}$ $CD1d^{hi}CD5^+$ phenotype, produce TGF-β, induce formation of regulatory $Foxp3^+$ T cells *in vitro*, and suppress development of AAD *in vivo* via enhanced accumulation of $Foxp3^+$ T cells in the airways. Further analysis of the genesis and function of these TGFβ-producing Bregs will help us understand how mice are capable of modulating their AAD and, thereby, yield potential insights into a cure for asthma.

METHODS

Ovalbumin animal model protocol

Female C57BL/6J mice were obtained from The Jackson Laboratory (Bar Harbor, ME). Animals were housed in the animal facility at the University of Connecticut Health Center and were treated in accordance with institutional and Office of Laboratory Animal Welfare guidelines. As previously described,[21–23] mice were immunized with 3 weekly intraperitoneal injections of 25 μg OVA in alum. One week after the last immunization, the mice are exposed to 1% aerosolized OVA in physiological saline, one hour/day for either 7 days (AAD) or 42 days (LIT), with an estimated inhaled daily dose of 30–40 μg/mouse.

Bronchoalveolar lavage (BAL)/tissue analysis

At sacrifice, BAL fluid, hilar lymph nodes, inguinal lymph nodes, and spleens were harvested and processed for the isolation and enumeration of leukocytes. For collection of BAL, lungs were lavaged *in situ* with five 1.0 ml aliquots of sterile saline. Lymph nodes and spleens were harvested and mechanically disrupted into single-cell suspensions, with lysis of splenic erythrocytes by TAC solution (9 parts 0.83% w/v NH_4Cl; 1 part 2.57% w/v Tris, pH 7.0). For all tissue samples, total nucleated cell counts were obtained using a hemocytometer with nigrosin dye exclusion as a measure of viability.

Antibodies and immunofluorescence reagents

The following monoclonal antibodies, either phycoerythrin (PE) or fluorescein isothiocyanate conjugated or unlabeled, were purchased from BD Pharmingen (San Diego, CA) and eBiosciences (San Diego, CA): CD3 (145-2C11), CD4 (RM4-5), CD5 (53-7.3), CD8 (53-6.72), CD19 (1D3), CD25 (PC61), B220 (RA3-6B2), CXCR4 (2B11), CXCR5 (2G8), Foxp3 (FJR-16s), IL-10 (JES5-16E3), IgD (11–26), and IgM (11/41). In addition, PE labeled anti-CD4 and anti-CD8 were purchased from Coulter Immunology (Marietta, GA). An anti-latency associated protein (LAP) of TGF-β was purchased from R & D Systems (Minneapolis, MN) and used to detect TGF-β bound to cells.

FACS analysis

Isolated lymphocytes were resuspended in PBS containing 0.2% BSA and 0.1% NaN_3 at a concentration of 1×10^5 to 1×10^6 white blood cells/ml, and 100 μl of the cells were incubated with 100 μl of properly diluted mAb at 4° C for 30 min. For the identification of $Foxp3^+$ Treg cells, cells stained with anti-CD3, anti-CD4, and anti-CD25 were permeabilized using fixation/ permeabilization buffer, following the manufacturer's protocol, and stained using anti-Foxp3-allophycocyanin (FJK-16s) with corresponding isotype controls (eBioscience, San Diego, CA). After staining, the cells were washed twice with PBS containing 0.2% BSA and 0.1% NaN_3 solution, and relative fluorescence intensities were measured on a 4-decade log scale by flow-cytometric analysis using a FACSCalibur or LSR II (Becton-Dickinson, San Diego, CA). For identification of CXCR4 and CXCR5 positive cells, cells were stained, incubated at 37° C for 45 minutes, washed in the above PBS solution, and samples were on Becton Dickinson LSR II.

For intracellular IL-10 staining, 1×10^6 cells from the Spleen or HLN were plated in a 96-well plate and treated with BD Golgi Plug® (BD Pharmigen). Cells were stimulated with phorbol 12-myristate 13-acetate (PMA) (50 ng/ml; Sigma-Aldrich, Inc.) plus ionomycin (1 μg/ml; Sigma-Aldrich, Inc.) or left unstimulated for 5 hours at 37°C.[29] Cells were then stained for surface cell markers, treated with Cytofix/perm buffer (BD Pharmigen), and followed by intracellular cytokine staining with α-IL-10 at 4°C. After staining all samples were run on LSR II and analyzed with FlowJo, Tree Star Inc., software.

Mice at the various stages were sacrificed on different days and hence the gating strategy was kept consistent for all tissues at a particular stage. This is shown by different sized quadrants in the dot plots in Figures 1, 5, 6. Selective representative dot plots are presented in each figure.

Confocal Microscopy

HLN were cryopreserved in OCT, sectioned, and stained as described previously.[47] In brief, frozen sections of thickness 20 μm were fixed in acetone or glutaraldehyde, washed in ice cold PBS, and stained for 60 minutes at room temperature with a combination of fluorescently conjugated Abs (anti-B220, anti-CD4, anti-Foxp3) in 2% normal goat serum and 2% FCS/PBS solution. For consistency, the middle sections from each node were used for staining. To detect Foxp3 positive cells, the sections were prepared and permeabilized according to instructions in the Foxp3 staining kit (eBiosciences, CA). The sections were then Fc blocked (anti CD16/CD32), stained with Foxp3 overnight at 4° C, washed, mounted and analyzed by confocal microscopy.

For quantification of $B220^+$ B cells and $Foxp3^+$ Tregs, the spots tool in Imaris suite was used. B cell zones were selected using boxes along the entire area of $B220^+$ cell clusters and T cell zones were selected boxes along the entire area based on the distribution of $CD4^+$ cells. The T-B border of 100μm thickness (50μm into the B cell zone and 50μm into the T cell zone) was selected using approximately four boxes of appropriate length and width along the border of B cell zone. The four boxes represent the T-B cell border for one follicular image. For every mouse, 3–4 such follicular areas were imaged, and there were 2 mice per group. $B220^+$ cells (green) and $Foxp3^+$ cells (red) were enhanced, and the spots were counted to obtain the total number of each cell population. The ratios were then calculated from these numbers. To calculate the density values, X, Y and Z dimensions were obtained from regions selected based on distribution of T cell and B cells. The density was calculated using the formula = number of Tregs in a specific compartment/(X × Y × Z) of that compartment, with Units = μm^{-3}

Treg cell induction assay

Freshly isolated $CD4^+CD25^-$ Teff cells were obtained from spleens of Naïve mice using magnetic bead isolation (Miltenyi Biotech), with >95% purity. These Teff cells (1×10^6) were cocultured for 5 days with viable irradiated (2600 Rad) $CD19^+$ $CD5^+$ or $CD5^-$ B cells from HLNs of LIT mice (1×10^6; isolated as above), soluble anti-CD3 (1 μg/ml), and anti-CD28 (1 μg/ml). The cultures were in RPMI 1640 supplemented with 10% FCS and 50 μM 2-ME in 24-well plates. After 5 days in culture, the cells were taken out from the wells, and the intracellular expression of Foxp3 was assessed on gated $CD4^+$ T cells. All studies were performed in triplicate.

B cell isolation and adoptive transfers

B cells from HLNs and spleens of LIT mice were positively selected using a mouse $CD19^+$ isolation kit (Miltenyi Biotech, Auburn, CA). The $CD19^+$ cells were then separated by immunofluorescent labeling and subsequent isolation utilizing a FACS-Vantage sorter into $CD5^-$ and $CD5^+$ subpopulations. Purified B cell subpopulations (0.2×10^6 $CD19^+CD5^+$ or 1.0×10^6 $CD19^+CD5^-$ cells) were injected by tail vein into sensitized animals 2 days prior to 7 days of OVA aerosol exposures. Different numbers of $CD19^+CD5^+$ and $CD19^+CD5^-$ cells were chosen for transfer to represent their relative proportions in the whole LN adoptive transfer studies.[21]

Statistical analysis

Data were expressed as mean ± standard error of mean values. Statistical comparisons between group means were made with ANOVA followed by Fisher's protected least significant difference test between possible pair-wise combinations of means (StatView 4.5; Abacus Concepts or JMP7; SAS Institute). In all comparisons, $p < 0.05$ was used to determine statistical significance.

Supplementary Material

Refer to Web version on PubMed Central for supplementary material.

ACKNOWLEDGEMENTS

This work was supported by NIH grants R21–AI079533 and R01–HL43573.

REFERENCES

1. Mosmann TR, Coffman RL. TH1 and TH2 cells: different patterns of lymphokine secretion lead to different functional properties. Annu. Rev. Immunol. 1989; 7:145–173. [PubMed: 2523712]
2. Ricci M, Ross O, Bertoni M, Matucci A. The importance of Th2-like cells in the pathogenesis of airway allergic inflammation. Clin. Exp. Allergy. 1993; 23:360–369. [PubMed: 8334535]
3. Till S, et al. IL-13 production by allergen-stimulated T cells is increased in allergic disease and associated with IL-5 but not IFN-gamma expression. Immunology. 1997; 91:53–57. [PubMed: 9203965]
4. Robinson DS, et al. Predominant TH2-like bronchoalveolar T-lymphocyte population in atopic asthma. N. Engl. J. Med. 1992; 326:298–304. [PubMed: 1530827]
5. Romagnani S. Immunologic influences on allergy and the TH1/TH2 balance. J. Allergy Clin. Immunol. 2004; 113:395–400. [PubMed: 14758340]
6. Xystrakis E, Boswell SE, Hawrylowicz CM. T regulatory cells and the control of allergic disease. Exp. Opinion Biol. Therapy. 2006; 6:121–133.
7. Larché M. Regulatory T cells in allergy and asthma. Chest. 2007; 132:1007–1014. [PubMed: 17873195]
8. Poulsen LK, Hummelshoj L. Triggers of IgE class switching and allergy development. Ann. Med. 2007; 39:440–456. [PubMed: 17852040]
9. Wolf SD, Dittel BN, Hardardottir F, Janeway CA. Experimental autoimmune encephalomyelitis induction in genetically B cell-deficient mice. J. Exp. Med. 1996; 184:2271–2278. [PubMed: 8976182]
10. Fillatreau S, Sweenie CH, McGeachy MJ, Gray D, Anderton SM. B cells regulate autoimmunity by provision of IL-10. Nat. Immunol. 2002; 3:944–950. [PubMed: 12244307]
11. Mizoguchi A, Mizoguchi E, Takedatsu H, Blumberg RS, Bhan AK. Chronic intestinal inflammatory condition generates IL-10-producing regulatory B cell subset characterized by CD1d up-regulation. Immunity. 2002; 16:219–230. [PubMed: 11869683]
12. Wei B, et al. Mesenteric B cells centrally inhibit CD4+ T cell colitis through interaction with regulatory T cell subsets. Proc. Natl. Acad. Sci. USA. 2005; 102:2010–2015. [PubMed: 15684084]
13. Lenert P, Brummel R, Field H, Ashman RF. TLR-9 activation of marginal zone B cells in lupus mice regulates immunity through increased IL-10 production. J. Clin. Immunol. 2005; 25:29–40. [PubMed: 15742155]
14. Tian J, Zekzer D, Hanssen L, Lu Y, Olcott A, Kaufman DL. Lipopolysaccharide-activated B cells down-regulate Th1 immunity and prevent autoimmune diabetes in nonobese diabetic mice. J. Immunol. 2001; 167:1081–1089. [PubMed: 11441119]

15. Gonnella PA, Waldner HP, Weiner HL. B cell-deficient (μMT) mice have alterations in the cytokine microenvironment of the gut-associated lymphoid tissue (GALT) and a defect in the low dose mechanism of oral tolerance. J. Immunol. 2001; 166:4456–4464. [PubMed: 11254701]
16. Parekh VV, Prasad DV, Banerjee PP, Joshi BN, Kumar A, Mishra GC. B cells activated by lipopolysaccharide, but not by anti-Ig and anti-CD40 antibody, induce anergy in CD8+ T cells: role of TGF-β1. J. Immunol. 2003; 170:5897–5911. [PubMed: 12794116]
17. D'Orazio TJ, Mayhew E, Niederkorn JY. Ocular immune privilege promoted by the presentation of peptide on tolerogenic B cells in the spleen. II. Evidence for presentation by Qa-1. J. Immunol. 2001; 166:26–32. [PubMed: 11123273]
18. Tsitoura DC, Yeung VP, DeKruyff RH, Umetsu DT. Critical role of B cells in the development of T cell tolerance to aeroallergens. Internat. Immunol. 2002; 14:659–667.
19. Mizoguchi A, Bhan AK. A case for regulatory B cells. J. Immunol. 2006; 176:705–710. [PubMed: 16393950]
20. Mauri C, Ehrenstein MR. The 'short' history of regulatory B cells. Trends Immunol. 2008; 29:34–40. [PubMed: 18289504]
21. Singh A, et al. Regulatory role of B cells in a murine model of allergic airway disease. J. Immunol. 2008; 180:7318–7326. [PubMed: 18490731]
22. Yiamouyiannis CA, et al. Shifts in lung lymphocyte profiles correlate with the sequential development of acute allergic and chronic tolerant stages in a murine asthma model. Am. J. Pathol. 1999; 154:1911–1921. [PubMed: 10362818]
23. Schramm CM, et al. Chronic inhaled ovalbumin exposure induces antigen-dependent but not antigen-specific inhalational tolerance in a murine model of allergic airway disease. Am. J. Pathol. 2004; 164:295–304. [PubMed: 14695342]
24. Swirski FK, Sajic D, Robbins CS, Gajewska BU, Jordana M, Stampfli MR. Chronic exposure to innocuous antigen in sensitized mice leads to suppressed airway eosinophilia that is reversed by granulocyte macrophage colony-stimulating factor. J. Immunol. 2002; 169:3499–3506. [PubMed: 12244139]
25. Sakai K, Yokoyama A, Kohno N, Hamada H, Hiwada K. Prolonged antigen exposure ameliorates airway inflammation but not remodeling in a mouse model of bronchial asthma. Int. Arch. Allergy Immunol. 2001; 126:126–134. [PubMed: 11729350]
26. Van Hove CL, Maes T, Joos GF, Tournoy KG. Prolonged inhaled allergen exposure can induce persistent tolerance. Am. J. Respir. Cell Mol. Biol. 2007; 36:573–584. [PubMed: 17218615]
27. Jungsuwadee P, Benkovszky M, Dekan G, Stingl G, Epstein MM. Repeated aerosol allergen exposure suppresses inflammation in B-cell-deficient mice with established allergic asthma. Int. Arch. Allergy Immunol. 2004; 133:40–48. [PubMed: 14646377]
28. Singh A, et al. Subcutaneous late phase responses are augmented during local inhalational tolerance in a murine asthma model. Immunol. Cell Biol. 2008; 86:535–538. [PubMed: 18458679]
29. Matsushita, T.; Tedder, TF. Identifying regulatory B cells (B10 cells) that produce IL-10 in mice. In: Cuturi, MC.; Anegon, I., editors. Suppression and Regulation of Immune Responses, Methods in Molecular Biology. Vol. 677. New York: Springer Science+Business Media; 2011. p. 99-111.
30. Berland R, Wortis HH. Origins and functions of B-1 cells with notes on the role of CD5. Annu. Rev. Immunol. 2002; 20:253–300. [PubMed: 11861604]
31. Cyster JG, et al. Follicular stromal cells and lymphocyte homing to follicles. Immunol. Rev. 2000; 176:181–193. [PubMed: 11043777]
32. Forster R, Mattis AE, Kremmer E, Wolf E, Brem G, Lipp M. A putative chemokine receptor, BLR1, directs B cell migration to defined lymphoid organs and specific anatomic compartments of the spleen. Cell. 1996; 87:1037–1047. [PubMed: 8978608]
33. Allen CD, et al. Germinal center dark and light zone organization is mediated by CXCR4 and CXCR5. Nat. Immunol. 2004; 5:943–952. [PubMed: 15300245]
34. Sebastiani S, et al. Chemokine receptor expression and function in CD4+ T lymphocytes with regulatory activity. J. Immunol. 2001; 166:996–1002. [PubMed: 11145678]
35. Lundy SK, Berlin AA, Martens TF, Lukacs NW. Deficiency of regulatory B cells increases allergic airway inflammation. Inflamm. Res. 2005; 54:514–521. [PubMed: 16389573]

36. Cariappa A, et al. The follicular versus marginal zone B lymphocyte cell fate decision is regulated by Aiolos, Btk, and CD21. Immunity. 2001; 14:603–615. [PubMed: 11371362]
37. Youinou P, Jamin C, Lydyard PM. CD5 expression in human B-cell populations. Immunol. Today. 1999; 20:312–316. [PubMed: 10379049]
38. Lemoine S, Morva A, Youinou P, Jamin C. Human T cells induce their own regulation through activation of B cells. J. Autoimmun. 2011; 36:228–238. [PubMed: 21316922]
39. Yanaba K, Bouaziz J-D, Haas KM, Poe JC, Fujimoto M, Tedder TF. A regulatory B cell subset with a unique $CD1d^{hi}CD5^{+}$ phenotype controls T cell-dependent inflammatory responses. Immunity. 2008; 28:639–650. [PubMed: 18482568]
40. Bouaziz JD, Yanaba K, Tedder TF. Regulatory B cells as inhibitors of immune responses and inflammation. Immunol. Rev. 2008; 224:201–214. [PubMed: 18759928]
41. Mangan NE, Fallon RE, Smith P, van Rooijen N, McKenzie AN, Fallon PG. Helminth infection protects mice from anaphylaxis via IL-10-producing B cells. J. Immunol. 2004; 173:6346–6356. [PubMed: 15528374]
42. Amu S, Saunders SP, Kronenberg M, Mangan NE, Atzberger A, Fallon PG. Regulatory B cells prevent and reverse allergic airway inflammation via FoxP3-positive T regulatory cells in a murine model. J. Allergy Clin. Immunol. 2010; 125:1114–1124. [PubMed: 20304473]
43. Wilson MS, et al. Helminth-induced $CD19^{+}CD23^{hi}$ B cells modulate experimental allergic and autoimmune inflammation. Eur. J. Immunol. 2010; 40:1682–1696. [PubMed: 20306466]
44. Noh J, et al. Characterisation of allergen-specific responses of IL-10-producing regulatory B cells (Br1) in cow milk allergy. Cell. Immunol. 2010; 264:143–149. [PubMed: 20646682]
45. Lee JH, et al. Allergen-specific transforming growth factor-β-producing CD19+CD5+ regulatory B-cell (Br3) responses in human late eczematous allergic reactions to cow's milk . J. Interferon Cytokine Res. 2011; 31:441–449. [PubMed: 21291325]
46. Carson WF IV, Guernsey LA, Singh A, Vella AT, Schramm CM, Thrall RS. Accumulation of regulatory T cells in the local draining lymph nodes of the lung correlates with the spontaneous resolution of a chronic model of murine asthma. Int. Arch. Allergy Immunol. 2008; 145:231–243. [PubMed: 17914275]
47. Khanna KM, Blair DA, Vella AT, McSorley SJ, Datta SK, Lefrançois L. T cell and APC dynamics in situ control the outcome of vaccination. J. Immunol. 2010; 185:239–252. [PubMed: 20530268]

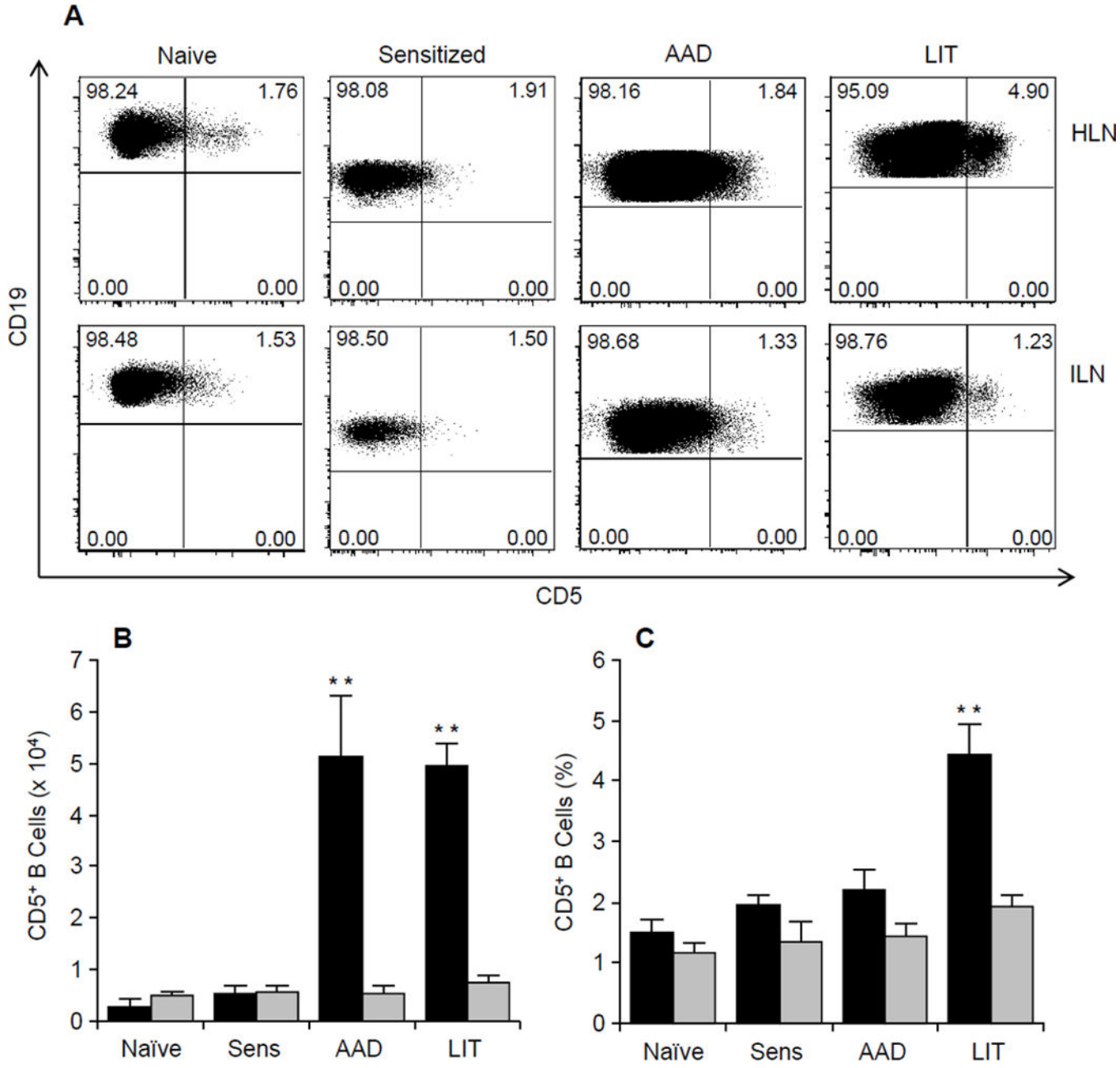

Figure 1. CD5$^+$ B cells were increased in the HLN at AAD and LIT

Cells were isolated from hilar (black bars) and inguinal lymph nodes (grey bars) at different stages of the OVA model (Naïve, Sensitized, AAD and LIT). Panel A depicts flow cytometry dot plots from representative tissues, and panels B and C show mean ± SEM values for total number (B) and percentage of CD5$^+$ B cells (C). Numbers of CD5$^+$ B cells were significantly expanded in hilar nodes at AAD and LIT, and they remained elevated as a percentage of total B cells during LIT. In contrast, no changes were seen in the inguinal nodes. n = 8–12 in each group. ** indicates $p < 0.005$ as compared to naïve and sensitized groups in hilar nodes and to all groups in inguinal nodes (Panel B), or $p < 0.005$ as compared to all other groups (Panel C).

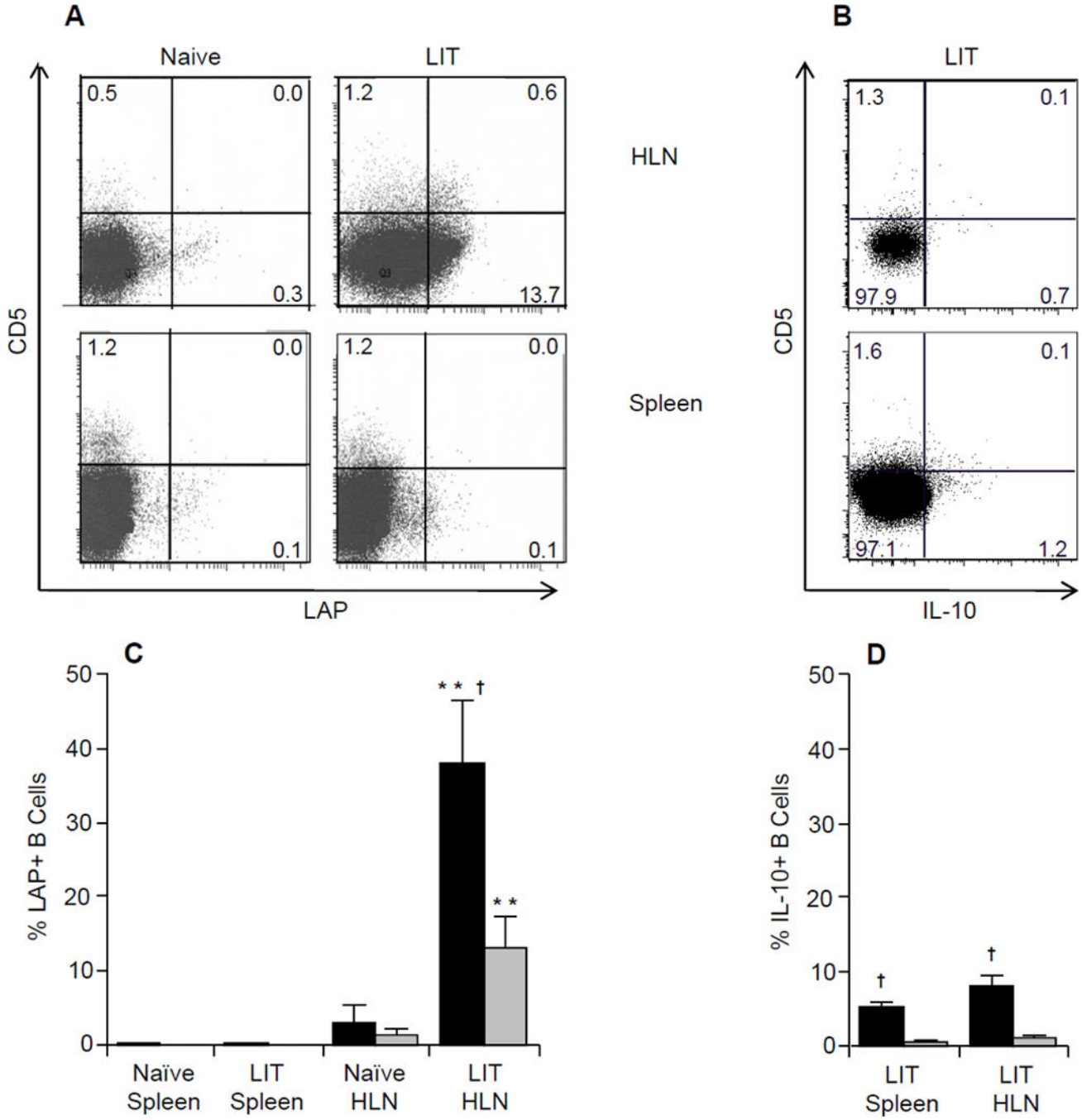

Figure 2. LAP and IL-10 expression in $CD5^+$ and $CD5^-$ B cells

Lymphocytes isolated from Spleens and HLN of Naïve and LIT mice were stained for B220, CD5, LAP, and IL-10, as described in the text. Panels A and B depict flow cytometry dot blots from representative tissues, and Panels C and D show mean ± SEM values for LAP expression (C) and IL-10 expression (D) in $CD5^+$ (black bars) and $CD5^-$ B cells (gray bars). **Panel C:** Relative to Naïve animals, LAP expression was unchanged in spleen $CD5^+$ and $CD5^-$ B cells of LIT mice, but LAP expression increased in HLN $CD5^+$ and $CD5^-$ B cells at LIT. **Panel D:** IL-10 levels were increased in $CD5^+$ B cells from both spleen and HLN

compared to $CD5^-$ B cells, but there was no difference in expression between LIT spleen and LIT HLN. $n = 4–5$ mice per group for LAP and 6 mice per group for IL-10 staining. ** indicates $p < 0.001$ from other groups by ANOVA; † indicates $p < 0.05$ for $CD5^+$ cells versus $CD5^-$ cells.

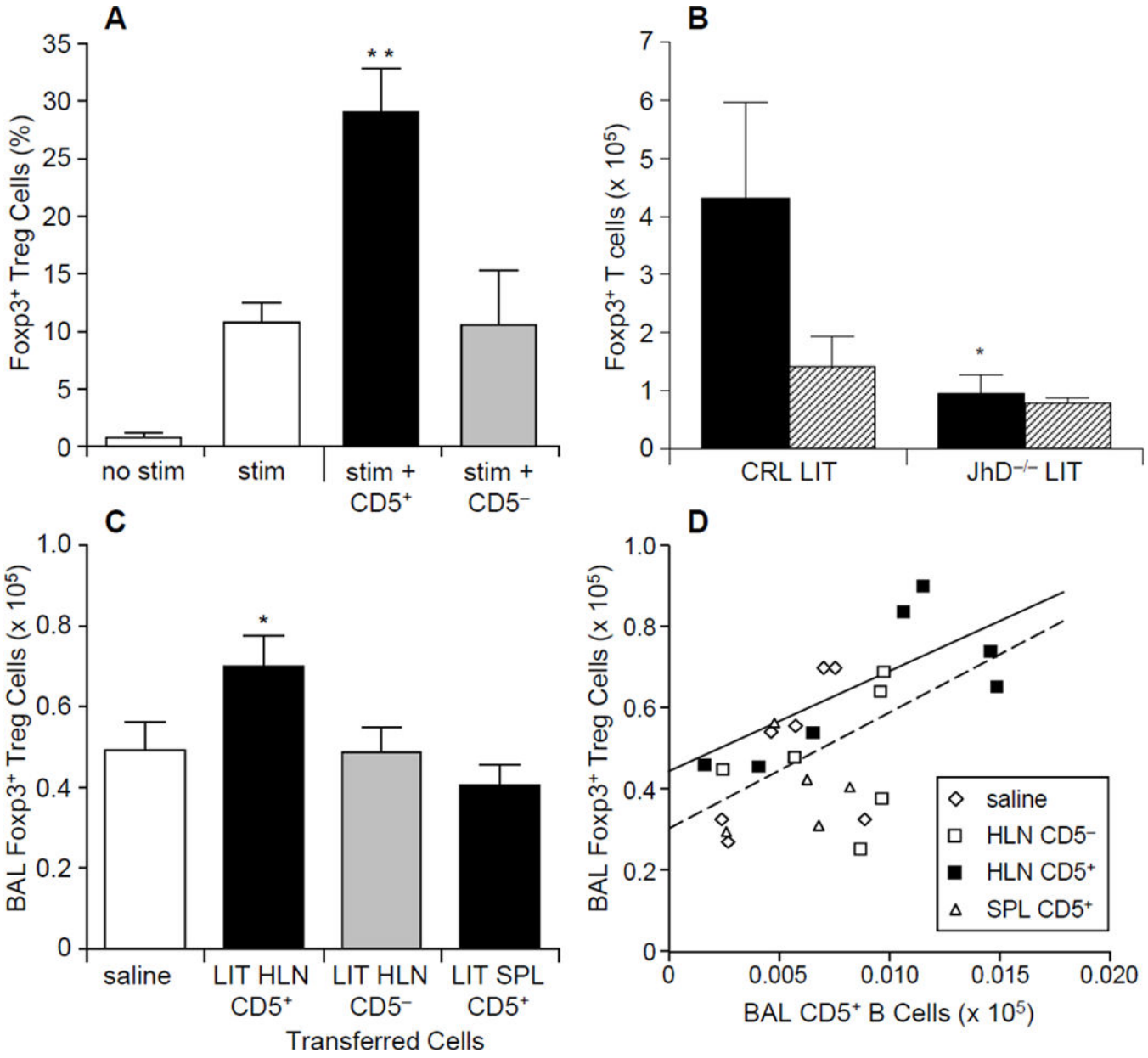

Figure 3. *In vitro* and *in vivo* dependence of Foxp3$^+$ Treg cells on CD5$^+$ B cells

Panel A: CD4$^+$CD25$^-$ T cells from spleens of naïve mice were co-cultured for 5 days without or with stimulation by soluble anti-CD3 and anti-CD28. Stimulated cells were also co-cultured with either irradiated CD19$^+$CD5$^+$ B cells or CD19$^+$CD5$^-$ B cells from LIT HLNs. T cell Foxp3 expression was increased when cultured with LIT HLN CD5$^+$ B cells versus with LIT CD5$^-$ B cells or anti-CD3/CD28 alone. Data represent mean ± SEM values of 3–4 animals per group; ** indicates $p < 0.01$ vs. other groups by ANOVA. **Panel B:** Foxp3$^+$ Treg expression was compared in LIT control and JhD$^{-/-}$ mice. Control mice showed expansion of Foxp3$^+$ Treg cells in hilar nodes (black bars) but not inguinal nodes (striped bars), but this local expansion did not occur in the JhD$^{-/-}$ mice. $n = 5$ mice per group; * indicates $p < 0.005$ between CRL and JhD$^{-/-}$ mice. **Panel C:** Two days before a

week of daily OVA aerosol exposures, OVA-sensitized mice received tail vein injections of saline or specific B cell populations. Mice receiving LIT HLN $CD5^+$ B cells demonstrated increased numbers of $Foxp3^+$ T cells in their BAL, as compared to control (saline) mice or mice receiving LIT HLN $CD5^-$ B cells or LIT spleen $CD5^+$ B cells. $n = 5–11$ mice per group; * indicates $p < 0.05$ vs. other groups by ANOVA. **Panel D:** For all groups of mice in panel C, there was a direct correlation between the number of $CD4^+Foxp3^+$ Treg cells and the number of $CD19^+CD5^+$ B cells in BAL (dashed line; $r = 0.56$; $p < 0.005$). This relationship also held for the LIT HLN $CD5^+$ recipient animals alone (solid line; $r = 0.73$; $p < 0.05$). In contrast, there was no association between $CD4^+CD25^+Foxp3^-$ Teff cells and $CD19^+CD5^+$ B cells in BAL ($r = 0.28$; $p > 0.10$; data not shown).

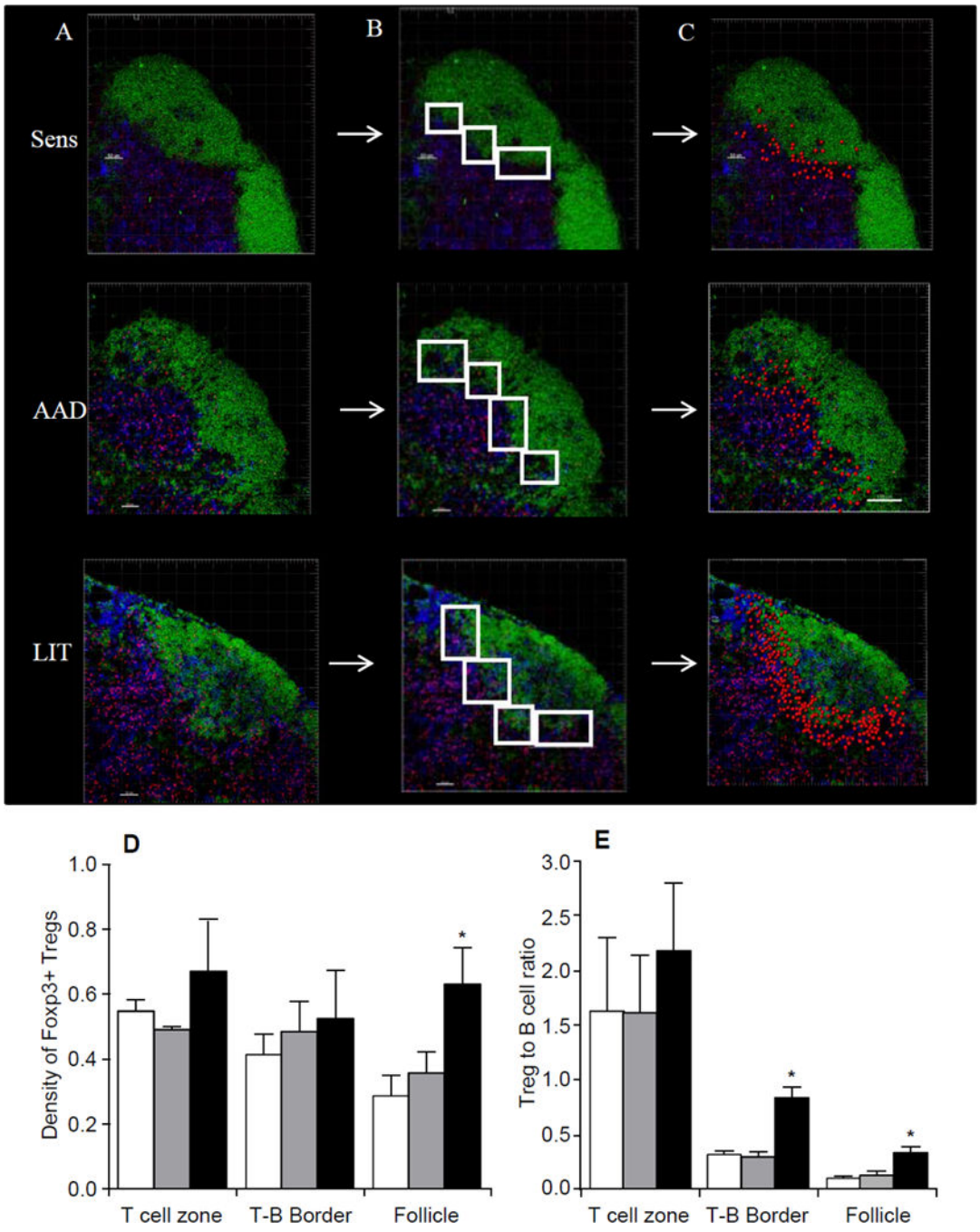

Figure 4. Increased Foxp3$^+$ Tregs in the follicular area of the HLN in mice at LIT via confocal microscopy

Confocal microscopy was performed on HLNs from mice after sensitization (white bars), at AAD (grey bars), and at LIT (black bars) to determine the locations of B cells and CD4$^+$Foxp3$^+$Treg cells. **Panels A–C:** Representative confocal images of HLNs from sensitized (upper panels), AAD (middle panels), and LIT mice (lower panels), with quantification assessed using Imaris software as described in methods. Regions of appropriate dimensions were selected along the T-B border for quantification of Foxp3$^+$ Tregs in that area (B). Foxp3$^+$ Tregs were enhanced using the spots tool in Imaris Suite (C)

and counted. Representative colors for confocal microscopy: green B220+ cells, blue $CD4^+$ cells, and red Foxp3+ cells. Images of magnification 20x. **Panels D–E:** Mean ± SEM values for $Foxp3^+$ Treg cell density (D) and the ratio of the number of Tregs to B cells (E) in the different HLN zones. $n = 6–8$ specimens per group; * indicates $p < 0.05$ as compared to sensitized and AAD in T-B border and B cell zone.

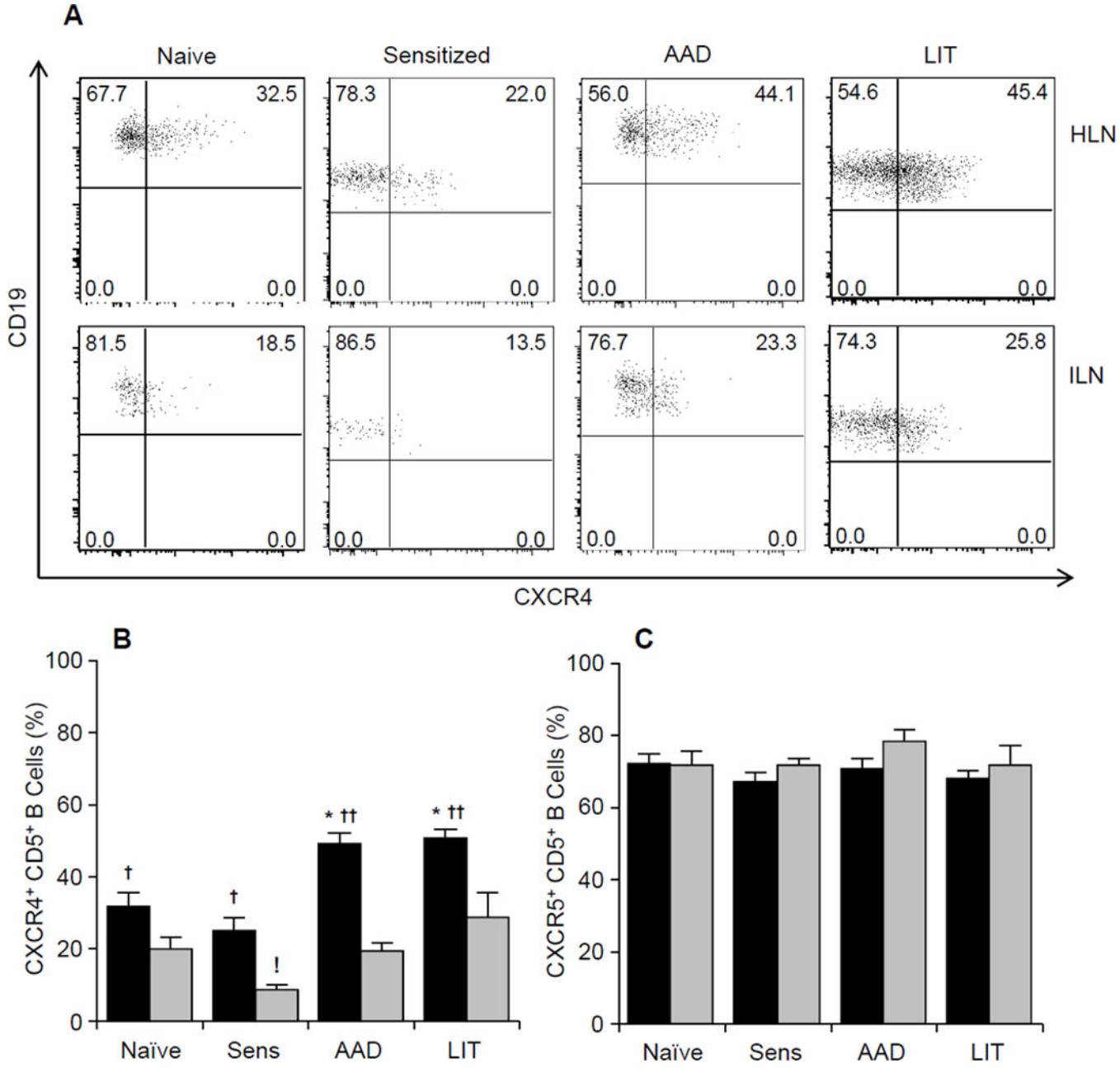

Figure 5. Hilar lymph node CD5$^+$ B cell expression of CXCR4 and CXCR5

CD5$^+$ B cells were isolated from hilar nodes (black bars) and inguinal nodes (gray bars) at different stages (Naïve, Sensitized, AAD and LIT) of the OVA model. **Panel A** depicts representative flow cytometry dot plots of CXCR4 expression on CD19$^+$CD5$^+$ B cells. **Panel B** demonstrates increased CXCR4$^+$CD5$^+$ B cells in hilar compared to inguinal lymph nodes at all stages of the model, and expansion of hilar node CXCR4$^+$CD5$^+$ B cells during AAD and LIT. **Panel C** demonstrates similar CXCR5 expression by CD5$^+$ B cells in both tissues and at all stages of the model. Data represent the mean ± SEM; n = 8–12 in each group (A, B); * indicates $p < 0.05$ as compared to Naïve and Sensitized groups in the HLN and to all groups in the ILN; ! indicates $p < 0.05$ as compared to all groups in the ILN; †

indicates $p < 0.05$ between HLN and ILN in Naïve and Sensitized groups; †† indicates $p < 0.005$ between HLN and ILN in AAD and LIT groups.

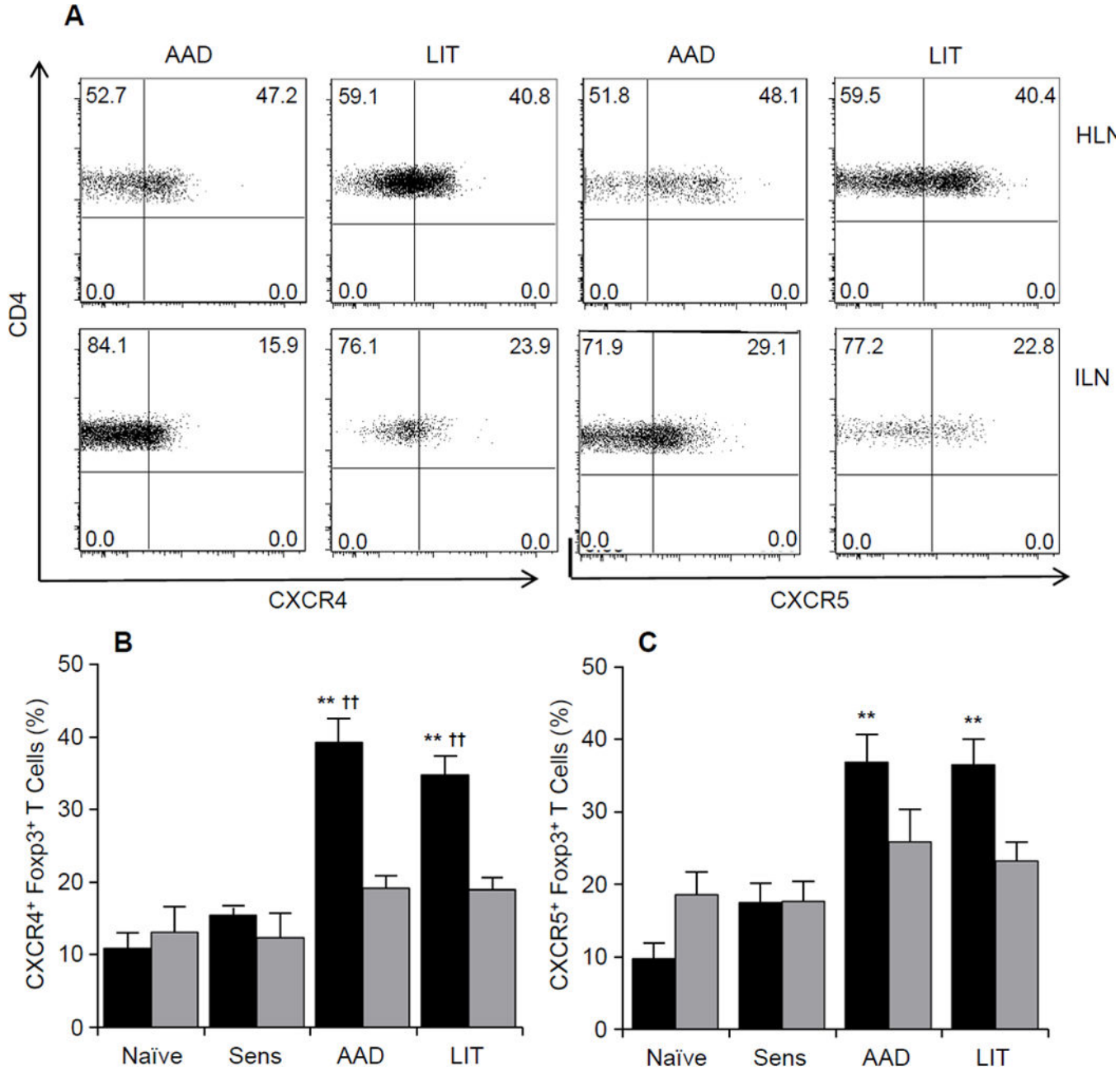

Figure 6. Hilar lymph node Foxp3$^+$ T cell expression of CXCR4 and CXCR5

Foxp3$^+$ T cells were isolated from hilar nodes (black bars) and inguinal nodes (gray bars) at different stages (Naïve, Sensitized, AAD and LIT) of the OVA model. **Panel A** depicts representative flow cytometry dot plots of CXCR4 and CXCR5 expression on CD4$^+$Foxp3$^+$ T cells. **Panel B** demonstrates increased CXCR4$^+$Foxp3$^+$ T cells in hilar compared to inguinal lymph nodes at AAD and LIT, and expansion of hilar node CXCR4$^+$Foxp3$^+$ T cells during AAD and LIT. **Panel C** demonstrates expansion of hilar node CXCR4$^+$Foxp3$^+$ B cells during AAD and LIT. Data represent the mean ± SEM; n = 4–8 in each group (A, B); ** indicates $p < 0.005$ as compared to Naïve and Sensitized groups in the HLN; †† indicates $p < 0.005$ between HLN and ILN in AAD and LIT groups.

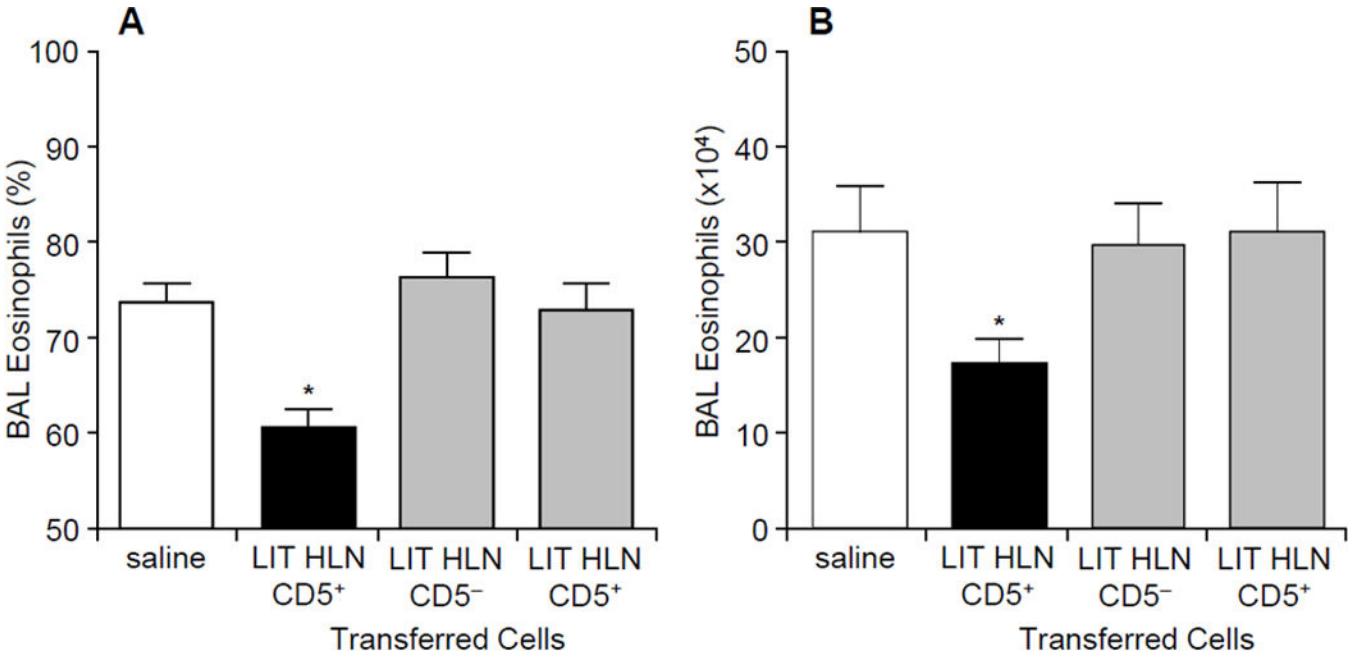

Figure 7. Attenuation of AAD by adoptive transfer of LIT HLN CD5$^+$ B cells into sensitized recipient mice

OVA-sensitized mice received tail vein injections of saline or specific B cell populations (0.2×10^6 CD19$^+$CD5$^+$ or 1.0×10^6 CD19$^+$CD5$^-$ cells) 2 days before a week of daily exposure to 1% OVA aerosols. Mice receiving the LIT HLN CD5$^+$ B cells (solid bars) developed attenuated AAD, with less relative (Panel A) and absolute (Panel B) airway eosinophilia relative to control (saline) mice or mice receiving LIT HLN CD5$^-$ B cells or LIT spleen CD5$^+$ B cells. Data represent mean ± SEM values of 5–11 mice per group; * indicates $p < 0.05$ vs. other groups by ANOVA.